Title

Improved data reduction for the deep-hole method of residual stress measurement

Journal

Journal of Strain Analysis for Engineering Design, 38(1)

ISSN

0309-3247

Authors

DeWald, Adrian T
Hill, Michael R

Publication Date

2003

Peer reviewed

Improved data reduction for the deep-hole method of residual stress measurement

A T DeWald and **M R Hill***
Mechanical and Aeronautical Engineering Department, University of California, Davis, California, USA

Abstract: This paper describes an improved data reduction scheme for the deep-hole method of residual stress measurement. The deep-hole method uses the changes in diameter of a reference hole, drilled through the thickness of a component, to determine residual stress. The diameter changes result from the removal of a cylindrical core from the component, where the core is larger than and concentric with the reference hole. The new data reduction seeks to determine the unknown eigenstrain distribution that gives rise to the residual stress state and to the reference hole deformations; once the eigenstrain distribution is found, it is input to an elastic finite element analysis to provide the residual stress distribution in the original component. The new data reduction relies on expressing the unknown eigenstrain field in a polynomial basis, and finding the unknown basis function amplitudes from the measured reference hole diameter changes. The new data reduction is compared with the current technique, and it is shown that the proposed scheme offers several advantages to the current method of data reduction.

Keywords: residual stress measurement, deep-hole method, eigenstrain, experimental mechanics

NOTATION

$\{A\}$	vector of coefficients of the eigenstrain polynomial series
$A(z), B(z)$	functions that account for the variations in reference hole strain with respect to z
$A_k^{xx}, A_k^{yy}, A_k^{xy}$	coefficients of the Legendre polynomial series for the eigenstrain components
$[C]$	compliance matrix relating reference hole strains to eigenstrain components
$d(\theta, z)$	measured reference hole diameter before core removal
$d'(\theta, z)$	measured reference hole diameter after core removal
d_o	nominal reference hole diameter
D	nominal outer diameter of the removed (trepanned) core
$\mathbf{D}$	isotropic elastic constitutive tensor
E	elastic modulus of the component material
$f(\theta, z), g(\theta, z), h(\theta, z)$	functions used in the approximate data reduction scheme
$[M(z_i)]$	matrix relating hole strains to residual stress components
$P_k(\zeta)$	Legendre polynomial of order k
r, θ	polar coordinates in the plane normal to the axis of the reference hole
r_o	half the nominal reference hole diameter $= d_o/2$
t	thickness of the residual stress-bearing component
x, y	coordinates in the plane normal to the axis of the reference hole
z	coordinate along the axis of the reference hole, through the depth of the component
z_i	depths where reference hole strains are measured
$\Delta d(\theta, z)$	change in reference hole diameter $= d'(\theta, z) - d(\theta, z)$
$\{\tilde{\varepsilon}\}$	vector of reference hole strains
$\tilde{\varepsilon}(\theta, z)$	reference hole strain $= \Delta d(\theta, z)/d_o$
$\{\tilde{\varepsilon}(z_i)\}$	vector of reference hole strains at depth z_i
$\varepsilon_{xx}^*, \varepsilon_{yy}^*, \varepsilon_{xy}^*$	eigenstrain components in the xy plane
$\tilde{\varepsilon}_\sigma$	approximate reference hole strain
$\boldsymbol{\varepsilon}$	total strain tensor
$\boldsymbol{\varepsilon}^*$	eigenstrain tensor
ζ	normalized through-thickness component $= 2z/t - 1$

The MS was received on 5 March 2002 and was accepted after revision for publication on 23 July 2002.
* *Corresponding author: Mechanical and Aeronautical Engineering Department, University of California, One Shields Avenue, Davis, CA 95616-5294, USA.*

θ_m	angles where reference hole strains are measured
v	Poisson's ratio of the component material
$\{\sigma(z_i)\}$	vector of residual stress components at depth z_i
$\sigma_{xx}, \sigma_{yy}, \sigma_{xy}$	residual stress components in the plane normal to the axis of the reference hole
$\boldsymbol{\sigma}$	stress tensor

1 INTRODUCTION

Residual stress can have a significant impact on material failure processes, and the ability to estimate residual stress is an important engineering tool. For thick steel components (e.g. thickness $t \geqslant 50$ mm), the deep-hole (DH) method is one of the few applicable methods for through-thickness residual stress measurement [**1**]. Because the method relies on the removal of only a small core of material, less than 20–50 mm in diameter, the measurement location can conceivably be weld repaired following residual stress measurement. A further advantage of DH is that the method can potentially be applied in the field; therefore structures need be removed from service only long enough to make the measurement and subsequent repair. Since the method has these positive attributes, further development of the DH method is desirable.

This paper introduces an improved data reduction scheme for determining residual stress from deformation measured in the DH experiment. As explained more fully below, current data reduction schemes rely on numerous assumptions [**2**, **3**] that may not be satisfied for a given application [**4**]. The reduction scheme presented here relies only on the assumptions of elastic stress release and stress state uniformity in the dimensions normal to the thickness, explicitly accounting for some of the factors that require additional assumptions in current schemes. The advantages of the new data reduction scheme are illustrated by comparing it with a current scheme, over a range of geometries and residual stress distributions.

1.1 Deep-hole method

The DH method estimates the through-thickness residual stress distribution in a component by measuring the change in diameter of a reference hole that occurs when a core of material is removed from the component by trepanning. The earliest references to the DH method appeared in 1978 [**5**, **6**], and the method has been used to determine residual stress in components up to 100 mm thick [**7**]. A schematic illustration of the DH method is shown in Fig. 1, and the steps in the DH method are as follows [**3**]:

1. A reference hole is gun drilled through the component (Fig. 1). The reference hole is polished to remove any abrupt changes in diameter.
2. Accurate measurements of the initial reference hole diameter are taken at a number of angles around the reference hole axis θ and at several increments of depth z (Fig. 1b), giving $d(\theta, z)$.
3. A core of material containing the reference hole is trepanned free of the rest of the component using a plunge electric discharge machine (Fig. 1c).
4. After core removal, the reference hole diameter is measured in the same manner as before (Fig. 1c, inset), giving $d'(\theta, z)$.
5. The changes in diameter of the reference hole are used to calculate the through-thickness distribution of residual stress in the component.

Further experimental details for the DH method were described by Leggatt *et al.* [**7**].

In presenting the methods for computing residual stress from the measured reference hole diameter, the notation in Fig. 2 is adopted, which defines the coordinate directions (x, y, z) and (r, θ, z), the core diameter D, the nominal reference hole diameter d_o and the component thickness t.

2 DATA REDUCTION TECHNIQUES

This paper describes a new method for finding residual stress from measured diameter changes. This new data reduction scheme takes as input the diameter changes, as a function of both angular orientation around the hole and depth from the surface, and provides the three residual stress components in the plane normal to the reference hole axis as a function of depth from the surface. The focus is on the in-plane residual stress components for simplicity; the distribution of the out-of-plane residual stress component could be added as an extension of the method. In order to highlight the differences between the new approach and other methods, one current calculation scheme for the DH method is presented first.

2.1 Approximate solution

The current method for determining the through-thickness residual stress distribution from DH experiments was presented by Leggatt *et al.* [**7**] and was further discussed by Smith *et al.* [**3**]. Although the original work includes the measurement of the through-thickness residual stress component, at present it is assumed that this stress component is negligibly small. This data reduction method takes the experimentally measured

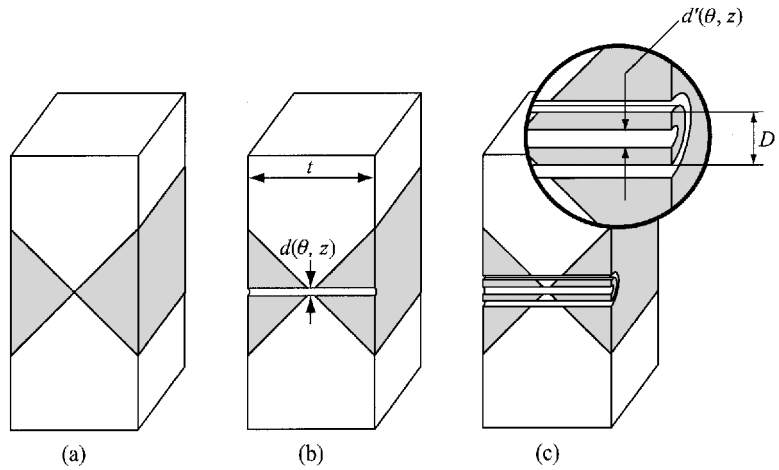

Fig. 1 Schematic illustration of the DH method

changes in reference hole diameter and converts them to strains by normalizing with the original reference hole diameter d_o. The change in the reference hole diameter, $\Delta d(\theta, z)$, is calculated according to

$$\Delta d(\theta, z) = d'(\theta, z) - d(\theta, z) \tag{1}$$

where d and d' are the reference hole diameters before and after trepanning respectively, which are each functions of the angular orientation around the hole, θ, and depth through the core thickness, z. The changes in reference hole diameter are then converted to strain using

$$\tilde{\varepsilon}(\theta, z) = \frac{\Delta d(\theta, z)}{d_o} \tag{2}$$

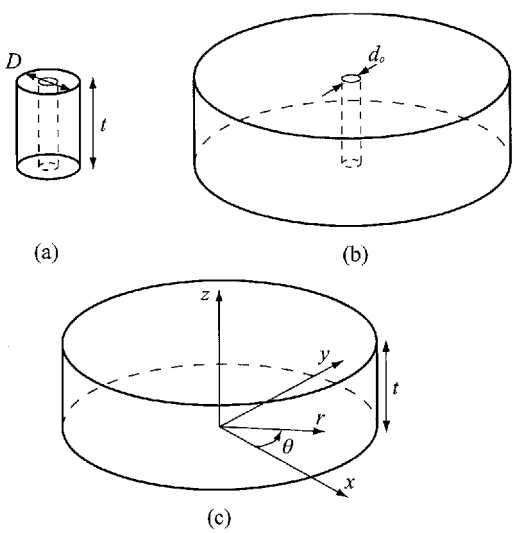

Fig. 2 Three geometries in the DH method: (a) trepanned core, (b) component with reference hole and (c) solid component

where d_o is the nominal reference hole diameter (and is independent of z).

The reference hole strains $\tilde{\varepsilon}(\theta, z)$ are related to the residual stress components in the plane normal to the reference hole axis, $\sigma_{xx}(z), \sigma_{yy}(z)$ and $\sigma_{xy}(z)$, through a simple elastic analysis. The analysis is based on deformations occurring at a hole in a finite-thickness planar-infinite plate subjected to remote planar stress components. In the analysis, the remote stresses are constant through the plate thickness but, because there are different conditions of thickness-direction constraint at different locations through the thickness, the near-hole deformation is dependent on z [**2**]. For a given applied remote stress constant with depth, the reference hole strain that would occur is given by

$$\tilde{\varepsilon}(\theta, z) = \frac{f(\theta, z)\sigma_{xx} + g(\theta, z)\sigma_{yy} + h(\theta, z)\sigma_{xy}}{E} \tag{3}$$

where the functions f, g and h were given by Garcia Granada *et al.* [**2**] as

$$f(\theta, z) = A(z)[1 + B(z)\ 2\ \cos(2\theta)] \tag{4}$$

$$g(\theta, z) = A(z)[1 - B(z)\ 2\ \cos(2\theta)] \tag{5}$$

$$h(\theta, z) = 4A(z)B(z)\ \sin(2\theta) \tag{6}$$

The functions $A(z)$ and $B(z)$ account for the variation in reference hole strain with z. Garcia Granada *et al.* [**2**] used finite element analysis to find $A(z)$ and $B(z)$ for a reference hole of 3.175 mm diameter in plates 20, 50 and 100 mm thick. $A(z)$ was found to be approximately 1 and independent of z, while $B(z)$ varied from about 0.85 near the plate mid-thickness to 0.98 near the surface (Fig. 3). To find residual stresses that vary with depth, it is assumed that the trepanned core is composed of a stack of annular slices, which act independently of one

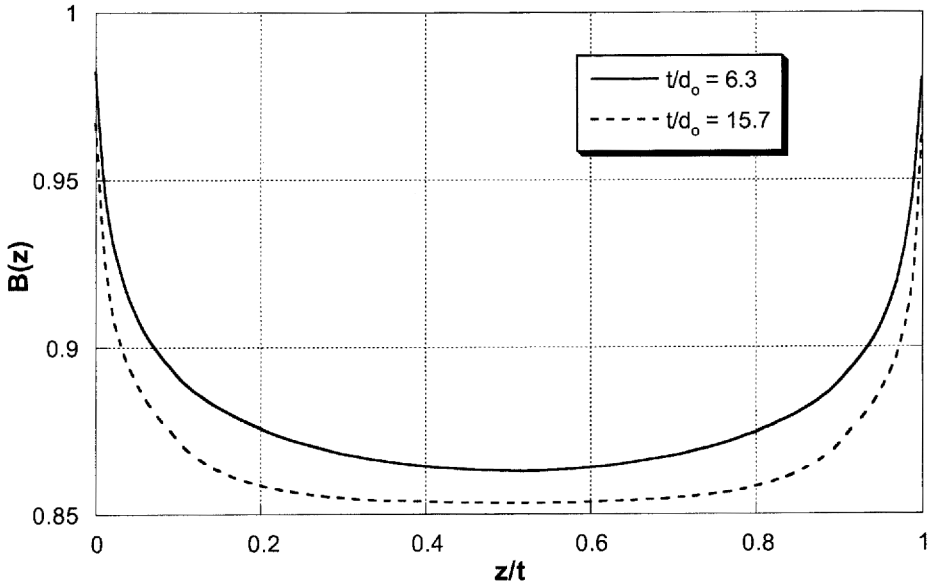

Fig. 3 $B(z)$ for a $d_o = 3.175$ mm reference hole in $t = 20$ and 50 mm plates [**2**]

another and behave in a manner predicted by the constant remote stress analysis.

A through-thickness residual stress distribution is calculated from measured reference hole strains $\tilde{\varepsilon}(\theta, z)$ through the use of a compliance matrix. Since the trepanned core is assumed to be composed of a stack of independent annular slices, stresses at a given depth are found independently from those at other depths. Reference hole strain is measured at a set of n depths $z = \{z_1, z_2, z_3, \ldots, z_n\}$ and a set of m angles $\theta = \{\theta_1, \theta_2, \theta_3, \ldots, \theta_m\}$, where $m \geqslant 3$. At each depth z_i, the measured strains are assembled into a vector of m components

$$\{\tilde{\varepsilon}(z_i)\} = [\tilde{\varepsilon}(\theta_1, z_i), \tilde{\varepsilon}(\theta_2, z_i), \ldots, \tilde{\varepsilon}(\theta_m, z_i)]^{\mathrm{T}} \tag{7}$$

The strain vector is then related to a vector of unknown stress components

$$\{\sigma(z_i)\} = [\sigma_{xx}(z_i), \sigma_{yy}(z_i), \sigma_{xy}(z_i)]^{\mathrm{T}} \tag{8}$$

through

$$\{\tilde{\varepsilon}(z_i)\} = -[M(z_i)]\{\sigma(z_i)\} \tag{9}$$

where the elements of the matrix $[M(z_i)]$ are derived from equations (3) to (6) and are given by

$$[M(z_i)] = \frac{1}{E}\begin{bmatrix} f(\theta_1, z_i) & g(\theta_1, z_i) & h(\theta_1, z_i) \\ f(\theta_2, z_i) & g(\theta_2, z_i) & h(\theta_2, z_i) \\ \vdots & \vdots & \vdots \\ f(\theta_m, z_i) & g(\theta_m, z_i) & h(\theta_m, z_i) \end{bmatrix} \tag{10}$$

Finally, the unknown stress components $\{\sigma(z_i)\}$ are calculated from the measured reference hole strains using least squares:

$$\{\sigma(z_i)\} = -\{[M(z_i)]^{\mathrm{T}}[M(z_i)]\}^{-1}[M(z_i)]^{\mathrm{T}}\{\tilde{\varepsilon}(z_i)\} \tag{11}$$

The analysis is repeated for all depths z_i, where the results at one depth are independent of those at the other depths.

A number of assumptions are made in this analysis, and these will have various impacts on the accuracy of the computed stresses. Firstly, the reference hole is assumed to have no impact on the stress released during trepanning. Secondly, the trepanned core is assumed to be free from stress. Thirdly, the trepanned core is assumed to be a stack of independently acting annular slices. Fourthly, the stress field is assumed to be independent of position normal to the reference hole axis. Fifthly, the deformation due to trepanning is assumed to be elastic. Each of these assumptions may have an impact on the accuracy of the stress computation scheme.

The reference hole diameter d_o and trepanned core diameter D can be selected to approximate certain assumptions of the data reduction scheme better. A small core diameter will minimize the amount of spatial averaging that occurs when the residual stress state varies with position normal to the reference hole axis. After trepanning, a core with a small diameter will also retain less residual stress than a core with a large diameter, the amount of retained stress depending on the curvature of the residual stress distribution with z [**8**]. For these two reasons, a small core diameter is desirable. If the reference hole diameter and the trepanned core diameter are of comparable size, however, the stress released during trepanning will be affected by the presence of the reference hole, therefore

invalidating an assumption of data reduction. This points to the need for a small reference hole diameter and a large core diameter. Further, a large core diameter is preferable to limit the effects of plasticity due to trepanning on the measured diameter changes. During trepanning, plasticity may arise due to the action of the cutting tool, due to the concentration of residual stress as the trepan is extended or due to a combination of these two effects. Attempts to select geometry to meet the assumptions of the data reduction scheme therefore lead to a trade-off between a small core diameter (which will minimize spatial averaging and will retain little residual stress) and a large core diameter (which will minimize the effects of the reference hole and of plasticity).

2.2 Eigenstrain series solution

2.2.1 General approach

An alternative formulation of the data reduction will now be described, which enables the experimenter to account for both residual stress released when the reference hole is drilled and for residual stress remaining in the trepanned core. The problem of finding residual stress in the region of the trepanned core is formulated by using an eigenstrain series solution. It is assumed that the residual stress does not vary with position normal to the reference hole axis, and that the deformations occurring during drilling of the reference hole and during trepanning are elastic. The solution scheme employs linear elastic finite element modelling, where the models include the actual geometries of the reference hole and trepanned core. The effects of the reference hole on stress released during trepanning and effects of stress retained in the trepanned core are properly accounted for.

The eigenstrain $\boldsymbol{\varepsilon}^*$ is a spatially varying inelastic tensor stain field that produces residual stress [**9**]. It enters an elastic stress analysis through the constitutive relation

$$\boldsymbol{\sigma} = \mathbf{D}(\boldsymbol{\varepsilon} - \boldsymbol{\varepsilon}^*) \tag{12}$$

where $\boldsymbol{\sigma}$ is the stress tensor, $\boldsymbol{\varepsilon}$ is the total strain tensor and $\mathbf{D}$ is the usual isotropic elastic constitutive tensor. The term in parentheses in equation (12) is the elastic strain. The usefulness of an eigenstrain formulation lies in the fact that, while trepanning alters the residual stress, it does not change the eigenstrain distribution provided that only elastic straining occurs; i.e., the *same* eigenstrain distribution causes *different* stress and deformation states in the geometries of interest. For the DH method, these geometries are as follows: Fig. 2a, trepanned core; Fig. 2b, infinite plate with the reference hole; Fig. 2c, original finite-thickness infinite plate. The differences between the stress states of these three geometries arise because of new traction-free surfaces created by cutting, thereby changing the equilibrium equations of elasticity. The measured reference hole strains are sufficient to determine the distribution with z of the eigenstrain components in the plane normal to the reference hole [i.e. $\varepsilon^*_{xx}(z), \varepsilon^*_{yy}(z)$ and $\varepsilon^*_{xy}(z)$]. With the eigenstrain components known, the residual stress in the plate, prior to drilling the reference hole, is then found by an elastic finite element analysis.

2.2.2 Determination of eigenstrain

It is assumed that each unknown component of eigenstrain is given by a Legendre polynomial series. For example, $\varepsilon^*_{xx}(\zeta)$ is given by a Legendre polynomial of degree l:

$$\varepsilon^*_{xx}(\zeta) = \sum_{k=0}^{l} A_k^{xx} P_k(\zeta) \tag{13}$$

where ζ is a normalized depth coordinate that runs from -1 to 1 as z runs from 0 to t, so that

$$\zeta = \frac{2z}{t} - 1 \tag{14}$$

and the $l+1$ coefficients A_k^{xx} of the polynomial series are to be determined. The same basis functions are used to express $\varepsilon^*_{yy}(\zeta)$ and $\varepsilon^*_{xy}(\zeta)$, but with additional corresponding coefficients A_k^{yy} and A_k^{xy} respectively. The Legendre polynomial of order $k+1$ can be found from the recurrence relation [**10**]

$$P_{k+1}(\zeta) = \frac{(2k+1)\zeta P_k(\zeta) - kP_{k-1}(\zeta)}{k+1} \tag{15}$$

where $P_0(\zeta)$ and $P_1(\zeta)$ are given by

$$P_0(\zeta) = 1 \tag{16}$$

$$P_1(\zeta) = \zeta \tag{17}$$

With the series representation of the unknown eigenstrain, the problem of determining the unknown eigenstrain distribution is reduced to finding the $3(l+1)$ coefficients A_k^{xx}, A_k^{yy} and A_k^{xy} of the three polynomial series for the eigenstrain components.

The coefficients of the three polynomial series are found from the reference hole strain measurements by solving an elastic inverse problem. To simplify the presentation, it is assumed for the moment that the unknown eigenstrain field consists only of $\varepsilon^*_{xx}(\zeta)$. The extension to the more general case where all three planar eigenstrain components are non-zero is made later. When only $\varepsilon^*_{xx}(\zeta)$ is non-zero, reference hole strains measured along a single orientation (e.g. $\theta = 0$) are sufficient to determine the coefficients A_k^{xx}. Assuming

elastic behaviour, the principle of superposition allows the expression of the reference hole strain as a linear combination of the unknown polynomial coefficients:

$$\tilde{\varepsilon}(\theta = 0, z_j) = \sum_{k=0}^{l} A_k^{xx} C_{jk} \tag{18}$$

where C_{jk} is the reference hole strain that would occur at depth z_j and $\theta = 0$ if the eigenstrain distribution were given exactly by $\overset{*}{\varepsilon}_{xx}(\zeta) = P_k(\zeta)$.

Because C_{jk} is the strain that occurs due to the *known* eigenstrain distribution $\overset{*}{\varepsilon}_{xx}(\zeta) = P_k(\zeta)$, it can be found by elastic analysis. Two elastic models are used to find C_{jk}, one of the infinite plate with reference hole (Fig. 2b) and one of the trepanned core (Fig. 2a). For each polynomial basis function, it is necessary to apply a corresponding eigenstrain distribution to each model, to solve for equilibrium and to record the deformed shape of the reference hole at $\theta = 0$ and at depths corresponding to those used in the physical measurements $z = \{z_1, z_2, z_3, \ldots, z_n\}$. Reference hole strains are then computed from these deformations using equations (1) and (2), with $d(\theta = 0, z_j)$ found from displacements on the model of the infinite plate with reference hole and $d'(\theta = 0, z_j)$ found from displacements on the model of the trepanned core. Repeating the analysis for all basis functions provides the elements of the matrix C_{jk} which has n rows (the number of depths) and $l + 1$ columns (the number of basis functions).

Provided that the number of depths, n, exceeds the number of assumed polynomial terms, $l + 1$, equation (18) can be solved in a least-squares sense for the unknown coefficients A_k^{xx} using an equation analogous to equation (11) (and given explicitly below).

For the case of three non-zero eigenstrain components, the analysis just described is extended to include additional unknown polynomial coefficients and additional angles of reference hole strain measurement. The extension from the case of a single eigenstrain component requires the careful organization of the reference hole strains and the polynomial coefficients. A vector representation for the reference hole strain is adopted:

$$\{\tilde{\varepsilon}\} = [\tilde{\varepsilon}(\theta_1, z_1), \tilde{\varepsilon}(\theta_1, z_2), \ldots, \tilde{\varepsilon}(\theta_1, z_n), \tilde{\varepsilon}\ (\theta_2, z_1), \tilde{\varepsilon}(\theta_2, z_2), \ldots, \tilde{\varepsilon}(\theta_3, z_n)]^{\mathrm{T}} \tag{19}$$

where $\theta_1 = 0$, $\theta_2 = \pi/4$ and $\theta_3 = \pi/2$ (although a different set of angles might be chosen such as $0, \pi/3$ and $2\pi/3$). A vector representation for the unknown coefficients of the eigenstrain polynomials is also adopted:

$$\{A\} = [A_0^{xx}, A_1^{xx}, A_2^{xx}, \ldots, A_l^{xx}, A_0^{yy}, A_1^{yy}, A_2^{yy}, \ldots, A_l^{yy}, A_0^{xy}, A_1^{xy}, A_2^{xy}, \ldots, A_l^{xy}]^{\mathrm{T}} \tag{20}$$

A linear system then relates the reference hole strain vector $\{\tilde{\varepsilon}\}$ to the polynomial coefficient vector $\{A\}$:

$$\{\tilde{\varepsilon}\} = [C]\{A\} \tag{21}$$

The matrix $[C]$ has $3n$ rows and $3(l + 1)$ columns, and the elements in the first n rows and $l + 1$ columns are the elements C_{jk} of equation (18) [i.e. they are the reference hole strains that occur at $\theta = 0$ at depth z_j when $\overset{*}{\varepsilon}_{xx}(\zeta) = P_k(\zeta)$]. The remaining $2n$ rows of the first $l + 1$ columns are filled with reference hole strains found from the elastic model on the angles θ_2 and θ_3. The remaining $2(l + 1)$ columns are filled by reference hole strains occurring when the polynomial basis functions of the eigenstrain components $\overset{*}{\varepsilon}_{yy}(\zeta)$ and $\overset{*}{\varepsilon}_{xy}(\zeta)$ are imposed in the elastic models. Given a vector of measured reference hole strain, $\{\tilde{\varepsilon}\}$, the unknown vector of basis function amplitudes $\{A\}$ is found using least squares from

$$\{A\} = ([C]^{\mathrm{T}}[C])^{-1}[C]^{\mathrm{T}}\{\tilde{\varepsilon}\} \tag{22}$$

With the vector of basis function amplitudes determined from the measured reference hole strains, the distribution of each of the three planar eigenstrain components is given by a known polynomial series, such as that for $\overset{*}{\varepsilon}_{xx}(\zeta)$ in equation (13).

2.2.3 *Determination of residual stress*

Residual stress is computed from the known distributions of the planar eigenstrain components by an elastic finite element analysis. The geometry for the analysis is that of the component without the reference hole, herein assumed to be an infinite plate (Fig. 1c). The three known eigenstrain component distributions are imposed simultaneously in an elastic model of this geometry. Solving for equilibrium in the presence of the eigenstrain components provides the desired residual stress state.

2.2.4 *Finite element implementation*

The elastic models required to form the matrix $[C]$ are formulated using the finite element method and analyses are performed using a commercial code [**11**]. The material model is linear elastic with anisotropic thermal expansion. Thermal expansion is used to introduce the eigenstrain fields [**12**, **13**], and the expansion components are given spatial distributions with z as required to impose the polynomial basis functions for each eigenstrain component. The stress and deformation states in a given geometry are found by imposing a unit temperature change and solving for equilibrium. Finite element meshes were designed to represent the three geometries of interest (Figs 4a to c). The meshes are three dimensional with 100 layers of elements along z, such that elements at the surfaces are five times smaller than

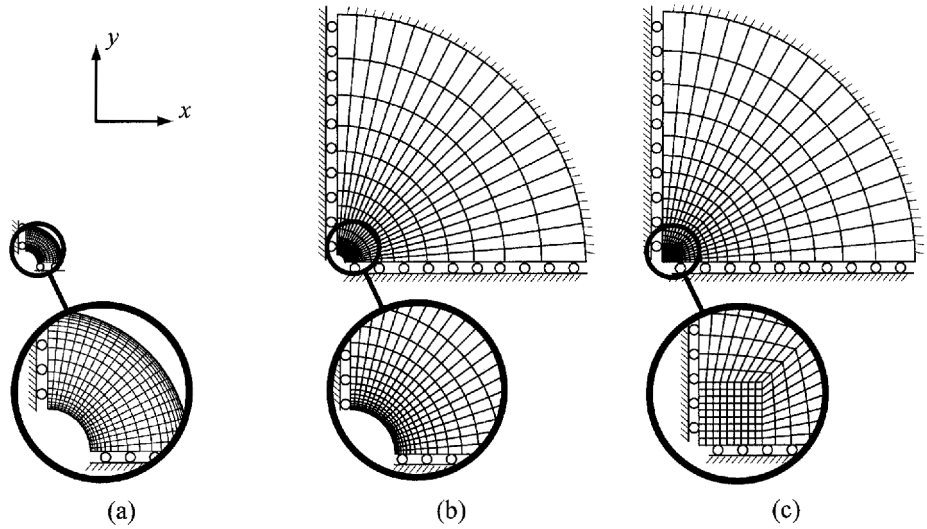

Fig. 4 Three quarter-symmetric models used in the eigenstrain analysis: (a) trepanned core, (b) component with reference hole and (c) solid component

those at the mid-depth of the model. Each mesh employed quarter-symmetry in the plane of the plate. The outside radius of the models of the infinite plate with and without the reference hole was approximately 30 times the reference hole radius, which was large enough to approximate an infinite geometry. These three finite element models are sufficient to simulate completely the DH measurement.

A tensor rotation was used to reduce the number of finite element simulations required to determine the elements of $[C]$. For a given geometry, reference hole deformations were determined for the basis functions of the xx component of eigenstrain using the quarter-symmetric finite element models. The deformations that would occur for the same basis functions but for the yy component of eigenstrain were then obtained from a coordinate rotation of the eigenstrain tensor by $\pi/2$ about the z axis, which results in

$$\tilde{\varepsilon}\left(\theta+\frac{\pi}{2},z\right)\Big|_{\varepsilon^*_{yy}} = \tilde{\varepsilon}(\theta,z)|_{\varepsilon^*_{xx}} \tag{23}$$

where the subscript on the trailing vertical bar reflects the eigenstrain component imposed when the reference hole strain occurs. Similarly, a coordinate rotation of the eigenstrain tensor about the z axis by $\pi/4$ provides deformations that would occur for the xy component of eigenstrain, so that

$$\tilde{\varepsilon}\left(\theta+\frac{\pi}{4},z\right)\Big|_{\varepsilon^*_{xy}} = 0.5[\tilde{\varepsilon}(\theta,z)|_{\varepsilon^*_{xx}} - \tilde{\varepsilon}(\theta,z)|_{\varepsilon^*_{yy}}] \tag{24}$$

The validity of these two equations was verified by performing developmental finite element simulations using fully cylindrical meshes, with no imposed symmetry conditions, and comparing the reference hole strains on $\theta = \pi/4$ and $\pi/2$ to strains computed using equations (23) and (24). This comparison showed agreement to four significant digits, as would be expected given the admissibility of the tensor rotation used to develop the above equations.

Equations (23) and (24) allow a significant reduction in effort when computing the elements of $[C]$. Firstly, they allow the use of a quarter-symmetric model in the plane normal to the reference hole. Since the deformation occurring when the xy eigenstrain fields are imposed is antisymmetric in the x and y directions, a fully symmetric model would be needed if the reference hole strains were not determined using equation (24). Secondly, the use of equations (23) and (24) allows a direct factor of three reduction in the number of cases analysed. Together, equations (23) and (24) provide a factor of 12 reduction in computational effort to determine the elements of $[C]$.

Finite element models were made for each of the three DH geometries. Quarter-symmetry of the models was enforced by restraining nodes in the xz and yz planes to remain within their respective initial planes. The mesh for the infinite plate with reference hole is shown in Fig. 4b. Nodes on the outer radius of this model were restrained from moving in the x and y directions in order to model the in-plane restraint imposed by the planar-infinite geometry. The outer radius of the mesh is approximately $30r_o$ where r_o is the radius of the reference hole. The outer radius of the model was found from convergence of the reference hole deformations with increasing outer radius, identified by constructing preliminary meshes with outer radii of approximately $10r_o$, $20r_o$ and $30r_o$. The mesh used for the trepanned core is shown in Fig. 4a. No restraints were placed on the nodes on the outer radius of the model, so that a traction-free surface would result. The mesh for the planar-infinite plate is shown in Fig. 4c. The outer radius of the model is the same as that used

for the plate with reference hole model (Fig. 4b), and nodes on the outer radius of the model are restrained in x and y to model the restraint of the planar-infinite plate. These models are employed to determine the elements of the matrix $[C]$ of equation (21) and to find residual stress once the eigenstrain amplitudes have been determined.

2.3 Comparison of methods

The two DH data reduction schemes are compared in two ways. In all analyses, the elastic material properties are taken to be $E = 207\,\text{GPa}$ and $v = 0.29$. For a given set of assumed DH geometry (i.e. d_o, D and t) and a given eigenstrain basis function, the finite element modelling provides a rigorous estimate of the reference hole strain due to trepanning, $\tilde{\varepsilon}(\theta, z)$, and this estimate is used as the foundation of the eigenstrain series solution. For comparison, a reference hole strain consistent with the assumptions of the approximate data reduction scheme is computed. This approximate reference hole strain is found from residual stress in the infinite plate caused by a given eigenstrain basis function and found from the finite element modelling. Substituting the components of residual stress at a particular depth into equation (9) provides an estimate of the reference hole strain consistent with the assumptions of the approximate data reduction scheme. This approximate reference hole strain will be referred to as $\tilde{\varepsilon}_\sigma(\theta, z)$, where the subscript σ signifies that the strain is computed from residual stress, using equation (9).

The first comparison of the two DH data reduction schemes is made by comparing $\tilde{\varepsilon}_\sigma(\theta, z)$ with $\tilde{\varepsilon}(\theta, z)$. If the diameter of the trepanned core is large compared with the diameter of the reference hole and the stress distribution is smooth, the two reference hole strains are expected to agree. To illustrate that the core size will cause differences between the approximate and eigenstrain approaches, a comparison is made between $\tilde{\varepsilon}_\sigma(\theta, z)$ and $\tilde{\varepsilon}(\theta, z)$ for a range of core sizes. To illustrate that the smoothness of the stress distribution also causes differences to arise, a comparison is made between $\tilde{\varepsilon}_\sigma(\theta, z)$ and $\tilde{\varepsilon}(\theta, z)$ over a range of polynomial basis functions, where higher-order basis functions vary more sharply than lower-order basis functions. In all calculations the reference hole diameter is $d_o = 6$ mm, which has been previously used in DH experiments [7]. Results are presented at $\theta = 0$ for the xx component of eigenstrain and for the thickness as $t = 50$ and 100 mm and core diameter $D = 10$ and 20 mm.

The second comparison of the two DH data reduction schemes illustrates the engineering significance of the difference between the two methods by simulating the application of DH to a plastically bent beam. In verifying their earlier data reduction scheme, Leggatt *et al.* [7] applied DH to a plastically bent beam 100 mm thick, 52 mm wide and 875 mm long. They used a 6 mm reference hole diameter and a 22 mm core diameter. To validate the DH measurement, Leggatt *et al.* estimated the expected through-thickness residual stress distribution in the beam by measuring strain at various points across the beam thickness during elastic–plastic beam bending. The strain data were then combined with a stress–strain curve and, assuming elastic unloading, the expected residual stress was computed. A close approximation to the expected axial residual stress is given by the trilinear distribution shown in Fig. 5.

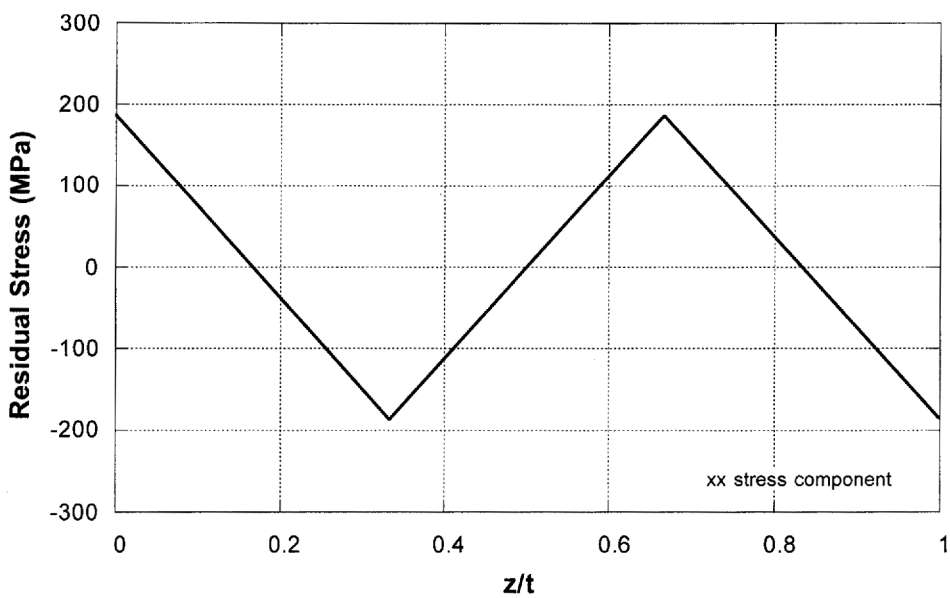

Fig. 5 Idealized residual stress in the plastically bent beam investigated by Leggatt *et al.* [7]

To simulate this DH application approximately, it is assumed that the initial geometry is an infinite plate (i.e. the finite beam width is not modelled), and the DH geometry has $t = 100$ mm and $D = 20$ mm. Reference hole strains that would occur in the presence of this stress field are found from finite element analysis by imposing the trilinear residual stress (Fig. 5) in the finite element models of the infinite plate with a reference hole (Fig. 4b) and the trepanned core (Fig. 4a) and solving for equilibrium. This stress state is introduced into the finite element modelling by assuming that it is uniaxial and by using the residual stress capability of the commercial code employed [**11**]. The deformations occurring in the two models are used with equation (2) to compute reference hole strains. These reference hole strains, occurring due to the input residual stress state, are then used as input to the data reduction schemes. A seventh-order polynomial series (i.e. $l = 7$) is used to represent the unknown eigenstrain components. The residual stress distributions determined by the approximate and eigenstrain data reduction schemes are then compared with the known residual stress state. To illustrate the degree to which the core diameter and plate thickness influence the stress determination, the simulation is repeated for $D = 20$ mm and $l = 50$ mm, for $D = 10$ mm, and $t = 50$ mm, and for $D = 30$ mm and $t = 100$ mm. The resulting errors in residual stress are plotted for each geometry and data reduction scheme, where the errors are the point wise differences between the input stress of Fig. 5 and the stress output by the data reduction schemes and where the errors are normalized by the peak input stress (187 MPa).

The approximate data reduction and the computation of approximate reference hole strains require values for $B(z)$ and these are taken from the values reported in reference [**2**] and plotted in Fig. 3. Since $B(z)$ is derived for a planar infinite geometry with thickness t and reference hole diameter d_o, the solution is characterized by the single non-dimensional parameter t/d_o with spatial distribution depending on relative depth z/t. The results in Fig. 3 are for $d_o = 3.175$ mm and $t/d_o = 6.3$ and 15.7. Over this fairly wide range of t/d_o the values of $B(z)$ vary by less than 3 per cent at any given value of z/t. For the present work, $d_o = 6$ mm with $t = 50$ and 100 mm ($t/d_o = 8.3$ and 16.7). Since $B(z)$ is insensitive to even sizeable variations in t/d_o, the $t/d_o = 6.3$ curve of Fig. 3 was used to provide $B(z)$ for the $t = 50$ mm case ($t/d_o = 8.3$) and the $t/d_o = 15.7$ curve was used for the $t = 100$ mm case ($t/d_o = 16.7$).

3 RESULTS

The reference hole strains $\tilde{\varepsilon}(\theta, z)$ and the approximate reference hole strains $\tilde{\varepsilon}_\sigma(\theta, z)$ are compared at $\theta = 0$ in Fig. 6 for three different eigenstrain basis functions $\varepsilon^*_{xx}(\zeta) = 0.001 P_k(\zeta)$ with $k = 1, 5$ and 9. The factor of 0.001 scaling the polynomials ensures reasonable levels of deformation in the analysis because residual stresses

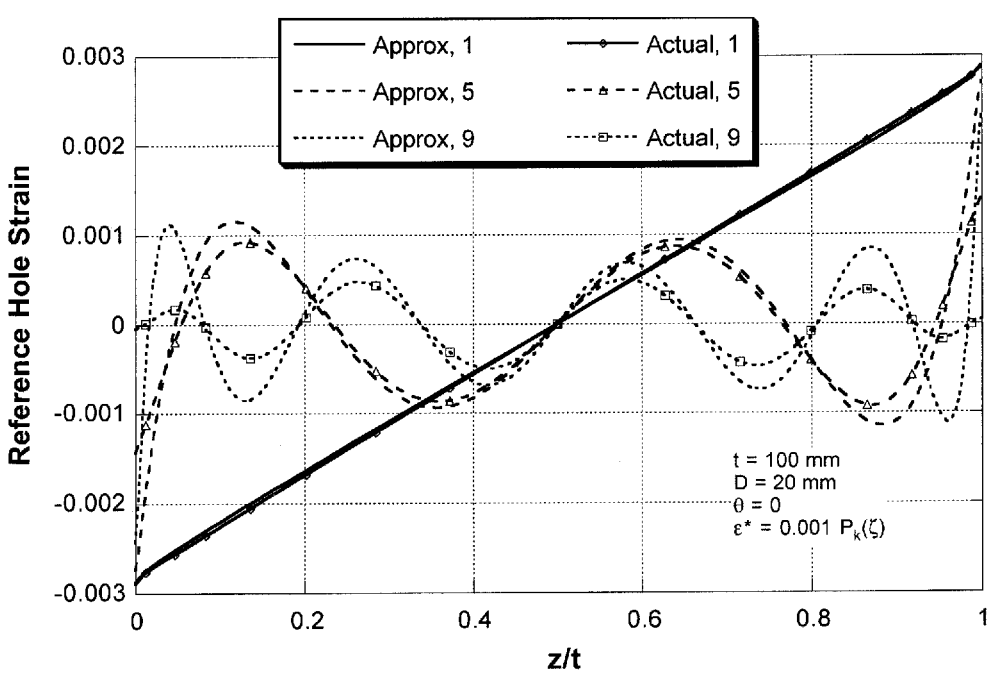

Fig. 6 Reference hole strains at $\theta = 0$ for $\varepsilon^*_{xx}(\zeta) = 0.001 P_k(\zeta)$ with $k = 1, 5$ and 9 and core dimensions $t = 100$ mm and $D = 20$ mm

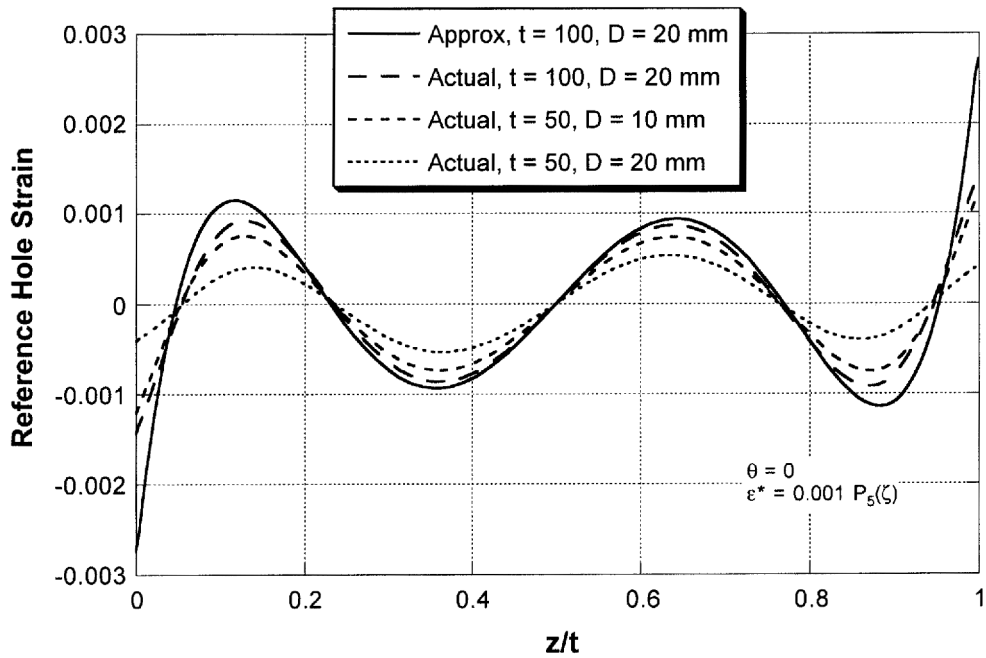

Fig. 7 Reference hole strains at $\theta = 0$ for various DH geometries with $\varepsilon^*_{xx}(\zeta) = 0.001P_5(\zeta)$

in engineering metals are of the order of 0.001 times the elastic modulus. The DH geometry modelled for the results in Fig. 6 is $t = 100$ mm and $D = 20$ mm. The reference hole strains $\tilde{\varepsilon}(\theta, z)$ are denoted 'actual' in the plot legend to reflect that they are a rigorous finite element estimate of deformations which would occur for the given eigenstrain distribution. The difference between the actual and approximate reference hole strains is small for low-order eigenstrain fields and becomes larger with increasing order. The difference in strain is probably due to residual stress remaining in the trepanned core, which is assumed to be zero in the approximate data reduction scheme.

The reference hole strain occurring at $\theta = 0$ for $\varepsilon^*_{xx}(\zeta) = 0.001P_5(\zeta)$ is shown in Fig. 7 for a range of core diameters D and component thicknesses t. Also shown in the figure is the approximate reference hole strain computed from residual stress. Results are presented in Fig. 7 for three different geometries: $t =$ 100 mm and $D = 20$ mm; $t = 50$ mm and $D = 20$ mm; $t = 50$ mm and $D = 10$ mm. The approximate reference hole strain is only plotted for $t = 100$ mm and $D = 20$ mm because it is independent of the core diameter and because the curve for $t = 50$ mm is indistinguishable from that for $t = 100$ mm [due to the similarity in $B(z)$ for these two thicknesses]. The actual reference hole strain depends significantly on both plate thickness and core diameter. The largest reference hole strain occurs for $t = 100$ mm and $D = 20$ mm, which has both the largest thickness and the smallest core diameter–thickness ratio $D/t = 0.2$. The smallest reference hole strain occurs for $t = 50$ mm and $D = 20$ mm, which has the smallest thickness and the largest core diameter–thickness ratio $D/t = 0.4$. The $t = 50$ mm, $D = 10$ mm, geometry shows that the reference hole strain depends on both the thickness t and on the core diameter–thickness ratio D/t, since the reference hole strain differs from the $t = 100$ mm, $D = 20$ mm, case but has the same D/t. Figure 7 also shows that the approximate method over-predicts deformation for all geometries considered, which probably occurs because the finite size core always retains some level of residual stress, thereby violating an assumption of the approximate reduction scheme. The fact that the approximate strain is an overestimate of deformation means that the approximate data reduction scheme will underestimate residual stress.

Simulation of the DH method for the case of the plastically bent beam shows that the accuracy of the approximate data reduction scheme depends on the core diameter and thickness employed. For a large thickness and small core diameter ($t = 100$ mm and $D = 20$ mm), the approximate and eigenstrain data reduction schemes produce comparable results (Fig. 8), with a small error in stress except near the peaks of the stress distribution (i.e. near $z/t = 0.33$ and 0.66). The error for the approximate data reduction scheme depends on the DH geometry (Fig. 9) while the error for the eigenstrain data reduction scheme does not (Fig. 10). The maximum error for the eigenstrain reduction scheme is 15 per cent of the peak stress for all geometries. The maximum error for the approximate reduction scheme ranges from 14 to 35 per cent of the peak stress, depending on D and t.

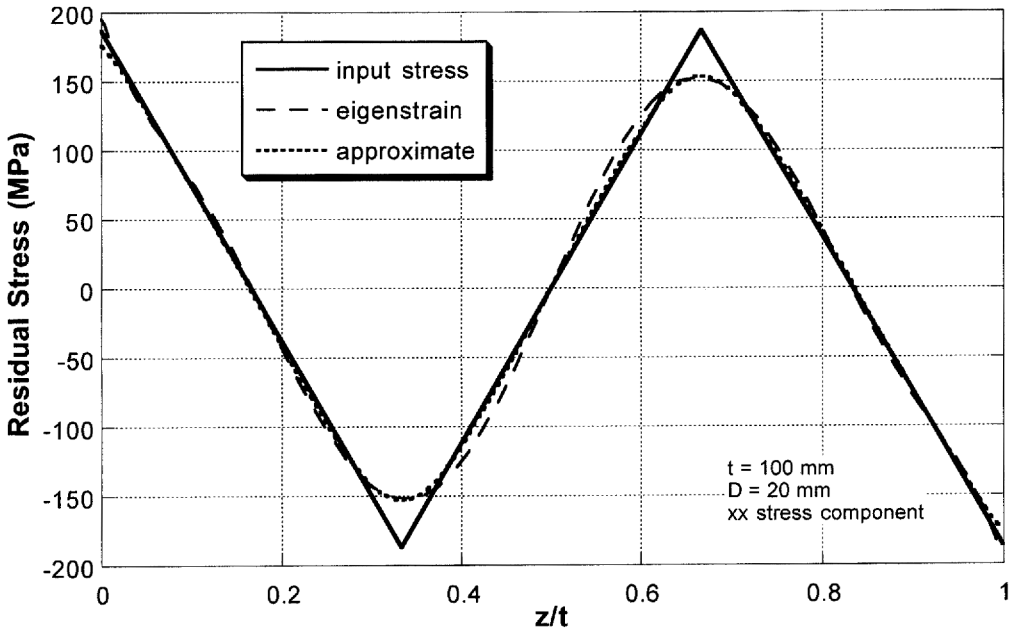

Fig. 8 Input and computed residual stresses for the plastically bent beam and core dimensions $t = 100$ mm and $D = 20$ mm

Error for the approximate data reduction scheme increases with D for constant t, and error decreases with t for constant D/t.

Even though the two reduction schemes produce stress errors for the bent beam that may be comparable (Fig. 8), the errors arise for different reasons. The error for the eigenstrain data reduction scheme arises due to the inability of the smooth polynomial basis functions to fit the sharply peaked residual stress distribution, an effect independent of the DH geometry (Fig. 10). The error in the approximate data reduction scheme is due to the differences between the actual reference hole strain and approximate reference hole strain. The increase in stress error with D/t at constant t and the decrease in error with t at constant D/t (Fig. 9) should be expected because the same trends are apparent in the difference between the actual and approximate reference hole strains (Fig. 7).

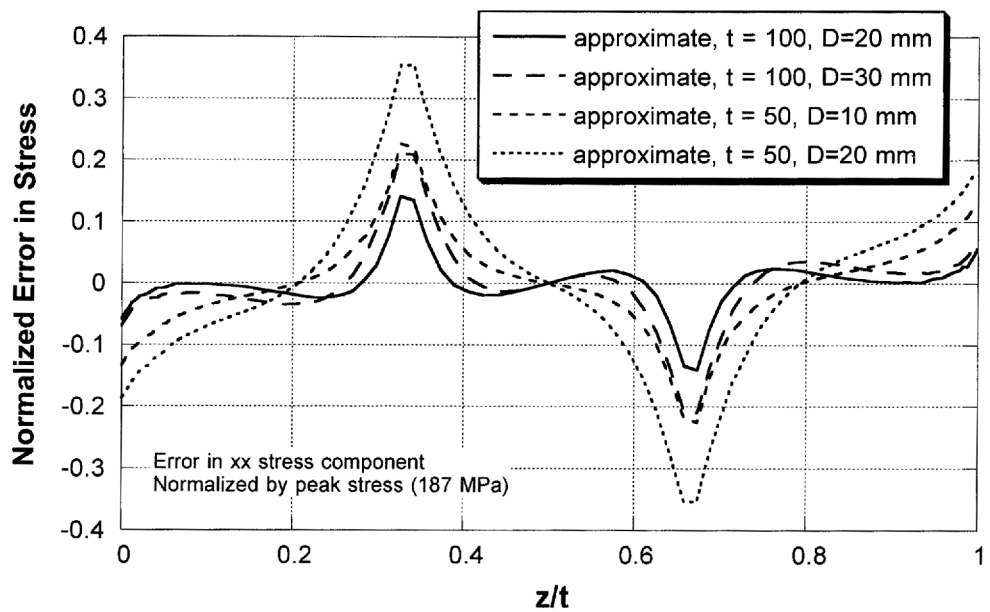

Fig. 9 Normalized error in residual stress in various DH geometries for approximate data reduction

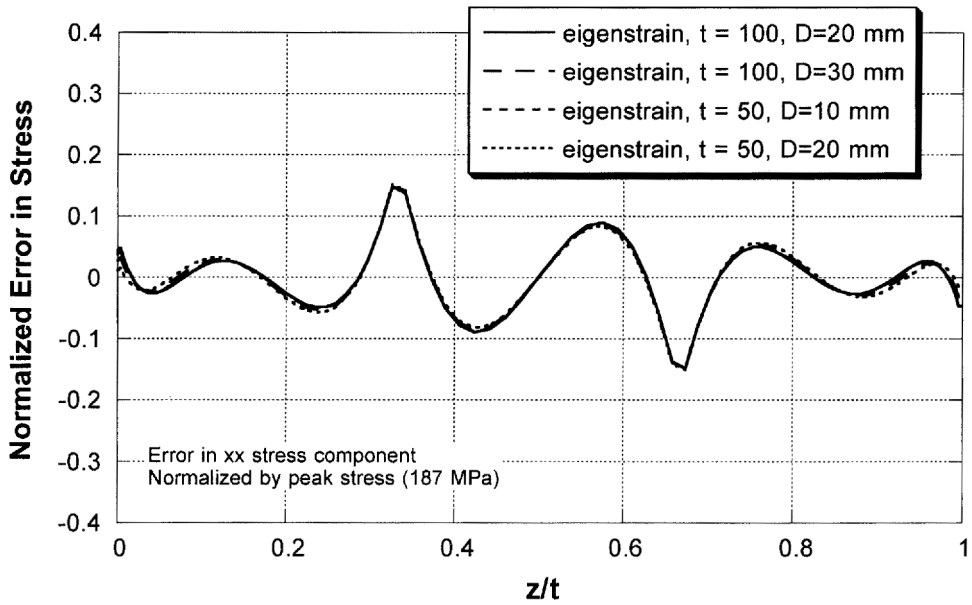

Fig. 10 Normalized error in residual stress in various DH geometries for eigenstrain data reduction

4 DISCUSSION

The mechanical performance of certain components can depend significantly on the residual stress present and, for such components, residual stress measurement is therefore required to assess structural integrity. Since the DH technique is one of the few methods capable of measuring residual stress deep within thick components, it is a valuable tool. To improve data reduction for the DH technique, this paper had two main objectives. The first of these was to develop a new method for computing residual stress from experimentally measured reference hole strains. The second objective was to compare the new method with previous data reduction schemes. Because the new method for stress computation relied on finite element modelling of the DH geometry, it accounted for the influences of component thickness and trepanned core diameter. Reference hole strains determined from finite element modelling were compared with those expected on the assumptions of a previous data reduction scheme and the comparison showed that the previous reduction scheme is prone to error for large core diameter or sharply varying eigenstrain fields. Application of the previous and eigenstrain data reduction schemes to the case of a plastically bent beam showed that both were capable of similar accuracy. However, while results from the eigenstrain data reduction were independent of the DH geometry, results from the previous scheme depend on geometry, potentially leading to large errors in residual stress.

A number of choices were made in developing the new data reduction scheme. The most fundamental of these was to seek the eigenstrain distribution rather than to seek the residual stress distribution directly. In principle, a stress-based approach would provide similar results, but using eigenstrain greatly simplified the analysis. Deformation due to cutting a residual stress-bearing body is most commonly modelled by applying tractions to cut surfaces, where the traction has equal magnitude and opposite direction to the (residual) stress vector referenced to the cut-plane normal at a given point. When the cut is perpendicular to a single normal residual stress component, as occurs in the slitting (crack compliance) method [**14**], applying tractions is relatively simple because the tractions are normal to the cut surface. For the trepanned core, however, the traction components would be oblique to the cut surface, therefore requiring the simultaneous application of normal and shear tractions at a given point on the surfaces of the trepanned core. Although this analysis is possible, the capability to apply surface shear tractions is absent from most commercial finite element codes. In comparison, the eigenstrain method relies on the anisotropic thermal expansion capability readily available in several commercial codes and, since the loading is generated at the integration points of the elements, the need to apply normal and shear tractions does not arise in the analysis.

A second choice made was the selection of a seventh-order Legendre polynomial series to express the spatial dependence of each of the unknown eigenstrain components. Legendre polynomials were selected over other polynomial series because they form an orthogonal basis, and because they have previously been used in other residual stress measurement applications (such as slitting [**14**]). Non-polynomial basis functions might have been selected to express the eigenstrain distribution

and may have produced better results for the case of the plastically bent beam. The bent beam stress distribution is difficult to fit using continuous polynomials because of the sharp peaks (Fig. 5), and this limits the ability of the eigenstrain data reduction to obtain better agreement in the near-peak region. Although the fitting is carried out for the eigenstrain distribution, the shapes of the eigenstrain and residual stress fields are similar. In fact, a direct seventh-order polynomial fit to the bent beam residual stress provides a stress distribution essentially equivalent to the result of the eigenstrain data reduction scheme (Fig. 8). It may be that a basis constructed from several piecewise linear or piecewise quadratic shape functions, distributing the eigenstrain components between several nodal locations, such as used in a one-dimensional finite element application, would provide improved results for stress in the near-peak region. Since the choice of basis functions is somewhat arbitrary, such a modification to the eigenstrain data reduction scheme is possible. However, analyses of other relaxation-based residual stress measurement methods indicate there are numerical advantages to using a polynomial basis, rather than piecewise functions (e.g. an analysis of hole drilling [**15**]).

The fact that the eigenstrain data reduction offers the same accuracy for a range of DH geometries is noteworthy. For the previous data reduction scheme, good accuracy is possible for some residual stress distributions provided that the proper geometry is selected. In the case of a constant or linear through-thickness stress distribution, the previous data reduction scheme will produce good results because the core will be essentially stress free. However, for other stress distributions, the accuracy will depend on the diameter of the core and the component thickness because the reference hole strains differ from those expected (Figs 6 and 7). Since the distribution of residual stress to be measured is often wholly unknown, the selection of the proper core diameter *a priori* is not possible. This problem is somewhat alleviated by the eigenstrain data reduction scheme because the relationship between reference hole strain and core geometry is accounted for, leading to accuracy that is independent of geometry (Fig. 10).

In comparing the two data reduction schemes a range of DH geometries that is representative of results in the literature was used, but recent work has focused on reducing the sizes of the reference hole and core. Recent work has used a DH geometry significantly smaller than that analysed here (e.g. $d_o = 3.175$ mm and $D = 10.0$ mm [**4**] and $d_o = 1.5$ mm and $D = 5.0$ mm [**16**]). For an arbitrary thickness, such smaller core diameters should improve the accuracy of the approximate data reduction scheme (Fig. 9).

The geometric independence of the eigenstrain data reduction scheme allows additional freedom in design of the DH experiment. As discussed previously, there are a number of considerations when selecting the diameters of the core and of the reference hole, and several of these remain important choices in applying the method. Because the eigenstrain data reduction offers the same accuracy for a range of core diameters (Fig. 10) and because the accuracy does not depend on the shape of the eigenstrain distribution, as it does for the previous data reduction scheme (Fig. 6), the choice of core diameter can be made on the basis of the anticipated effects of in-plane averaging (small core diameter) and of plasticity (large core diameter).

One additional advantage of the eigenstrain data reduction scheme is that it can be applied to a geometry that is more complicated. Here, the initial geometry was that of a flat plate and the removed core was a circular cylinder. In practice, measurements are also needed in parts containing curvature, a simple example being an initial geometry of a thick-walled tube, and a removed core taken radially that is cylindrical but has curved top and bottom surfaces (one being convex and the other concave). In such cases, the deformations due to core removal may be influenced by the top and bottom surface curvatures, with an unknown effect on the reference hole strains. The approach to data reduction presented here could be followed for such cases provided that the finite element models analogous to those in Fig. 4 reflect the actual geometries involved.

ACKNOWLEDGEMENTS

The authors gratefully acknowledge helpful consultations with Professor David Smith and Dr Daniel George of the University of Bristol, UK. Financial support for the project was provided in part by the Los Alamos National Laboratory, USA (agreement 32390-001-01 49), and by the GANN fellowship program of the US Department of Education.

REFERENCES

1 **Lu, J., James, M.** and **Roy, G.** *Handbook of Measurement of Residual Stresses*, 1996 (Fairmont Press).
2 **Garcia Granada, A. A., George, D.** and **Smith, D. J.** Assessment of distortions in the deep hole technique for measuring residual stress. In Proceedings of the 11th Conference on *Experimental Mechanics*, Oxford, 1998, pp. 1301–1306.
3 **Smith, D. J., Bouchard, P. J.** and **George, D.** Measurement and prediction of residual stresses in thick-section steel welds. *J. Strain Analysis*, 2000, **35**(4), 287–305.
4 **George, D.** Measurement of residual stress in thick section welds. PhD thesis, University of Bristol, 2000.
5 **Beaney, E. M.** Measurement of sub-surface stress. Report RD/B/N4325, Central Electricity Generating Board, July 1978.

6 **Zhdanov, I. M.** and **Gonchar, A. K.** Determining the residual welding stresses at a depth in metal. *Autom. Weld*, 1978, **31**(9), 22–24.

7 **Leggatt, R. H., Smith, D. J., Smith, S. D.** and **Faure, F.** Development and experimental validation of the deep hole method for residual stress measurement. *J. Strain Analysis*, 1996, **31**(3), 177–186.

8 **Hill, M. R.** Determination of residual stress based on the estimation of eigenstrain. PhD thesis, Stanford University, 1996.

9 **Mura, T.** *Micromechanics of Defects in Solids*, 2nd revised edition, 1991 (Kluwer, Boston, Massachusetts).

10 **Greeberg, M. D.** *Foundations of Applied Mathematics*, 1978 (Prentice-Hall, Englewood Cliffs, New Jersey).

11 *ABAQUS/Standard v.5.8*, 1999 (Hibbitt, Karlsson, and Sorenson, Providence, Rhode Island).

12 **Hill, M. R.** and **Nelson, D. V.** The inherent strain method for residual stress determination and its application to a long welded joint. In *Structural Integrity of Pressure Vessels, Piping, and Components—1995*, PVP Vol. 318, 1995, pp. 343–352 (American Society of Mechanical Engineers, New York).

13 **Matos, C. G.** and **Dodds Jr, R. H.** Modeling the effects of residual stresses on defects in welds of steel frame connections. *Engng Structs*, 2000, **22**(9), 1103–1120.

14 **Prime, M. B.** Residual stress measurement by successive extension of a slot: the crack compliance method. *Appl. Mechanics Rev.*, 1999, **52**(2), 75–96.

15 **Schajer, G. S.** and **Altus, E.** Stress calculation error analysis for incremental hole-drilling residual stress measurements. *Trans. ASME, J. Engng Mater. Technol.*, 1996, **118**(1), 120–126.

16 **George, D., Kingston, E.** and **Smith, D. J.** Measurement of through-thickness stresses using small holes. *J. Strain Analysis*, 2002, **37**(2), 125–139.

